Dynamics of shear bands in a dense granular material forced by a slowly moving rigid body

Eugenio Hamm and Francisco Melo
Departamento de Física de la Universidad de Santiago de Chile and
Center for Advanced Interdisciplinary Research in Materials (CIMAT)
Av. Ecuador 3493, Casilla 307 Correo 2, Santiago, Chile.
(Dated: April 20, 2007)

We measure the flow field in plane geometry around a slowly moving rigid finger that penetrates a dry randomly packed granular medium vertically. With the use of an image correlation technique we identify a localized flow around the finger limited by two well defined shear bands that nucleate below the tip of the finger and reach the free surface. Evolution of the shear bands is discontinuous, exhibiting nucleation-relaxation processes as the finger moves downwards. We present a simple model accounting for the shape of the shear bands. We measure the force applied by the finger and the sources of dilation as well.

PACS numbers: 45.70.-n, 47.57.Gc, 47.80.Cb

Since the early works of Coulomb and Faraday, granular materials have been recognized as a source of a rich variety of collective phenomena reminiscent of macroscopic behavior in solids, liquids and gases [1, 2]. Being now a subject of intense fundamental research and despite the efforts to understand their striking properties, most predictive models for the statics and dynamics of granular materials remain phenomenological, particularly in the case of dense slow flows. It is an experimental fact that granular compacts are prone to separate in space in metastable states when submitted to external forcing. In such states the stress field forms a grain-grain contact network that has no equivalent in continuous elastic systems. One of the main features of dense flow is the formation of yield surfaces where velocity gradients focus and the material dilates [3]. Outside these interfaces the flow is smooth and may be purely translational or rotational if aggregates of beads are in closely packed states. A fundamental problem is the slow motion of a rigid body in a dense granular material [4, 6, 7]. For instance, in [5], the authors study in detail the force applied to a flat disk that penetrates a granular material, particularly when it approaches a rigid bottom. However, observations of the flow and its correlation with the force applied to the disk seem difficult to achieve, due to the three dimensional features of the flow. A related case is found at later stages of crater formation resulting from high speed impacting objects [8].

From the experimental point of view, the study of granular flows encounters serious difficulties. For instance, the opaque nature of common granular materials and the long range of stresses they develop impose strong restrictions on bulk flow visualization and non-invasive probing, respectively [9]. Some of these difficulties have been overcome by noninvasive magnetic resonance methods [10] and laser sheet techniques [11].

In this letter we study experimentally the quasistatic flow field around a moving object in a granular medium.

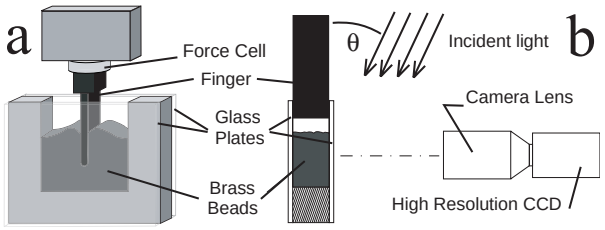

FIG. 1: a) Cell containing the granular material and b) lateral view of the setup.

In the experiment, we force a rigid finger to penetrate vertically a granular compact from its free surface. To visualize flow, we confine the material in a cell having two transparent walls through which we perform flow characterization. Our choice of a finger over other shapes obeys to the need of model experiments [12, 13] to develop more analytical understanding. In this configuration the granular material experiences a two dimensional flow which is characterized by two shear bands that evolve in a non-stationary way if viewed from the reference frame of the moving finger. We identify the geometrical features of the shear bands and we propose a mechanism that predicts their shape and evolution.

In our experiment the granular material consists of spheroidal brass beads of size $38\ \mu m \lesssim d \lesssim 63\ \mu m$, which are contained in a cell of dimensions 40(W)x 30(H) x 10(T) mm^3 (fig. 1a). The front and back walls of the cell are made of glass, 3 mm thick. The cell is filled up to a height of 20 mm by passing the granular flow across four successive fine metallic grids. To obtain a flat free surface we carefully tilt the cell in order to provoke small avalanches. The metallic finger is rectangular in section, has a semi-circular tip of radius $R = 1.5mm$ and a thickness equal to the gap between the glass plates (fig. 1b). It is fixed on a PC-driven submicron translation stage (Thorlabs T25X) for positioning, whereas the whole system is mounted on an optical table.

We measure the flow field via image cross-correlation at the interface between the granular material and the inner surface of the front glass plate. Low angle illumination and imaging are provided by a fiber-lite quartz-halogen lamp (fig. 1b) and a digital 12 Mpix camera (Nikon DXM 1200), respectively. The flow field is extracted by scanning the total image with a window of size $1mm^2$ that moves vertically/horizontally by steps of 0.25 mm. The method gives a direct measure of the macroscopic velocity field of the cluster of beads contained in the window. The finger is forced to move downwards at constant speed $\nu = 1.2\ \mu m/sec$, which is small enough to assure the quasistatic hypothesis. We measure the penetration depth of the finger by the position, ζ, of the tip of the finger, relative to the initially flat free surface. Images are taken "on the fly" each $\delta t = 20s$, with an exposure time of $1s$. In all our experiments we observe that the flow near the finger involves speeds of the order of ν, hence during time δt the beads move by distances smaller than the beads' size. This is important to preserve image correlation.

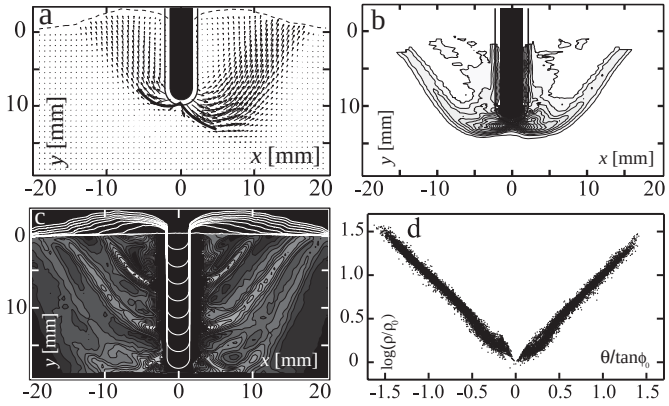

FIG. 2: a) and b) Quasistatic flow field around finger (in black) in plane geometry. Solid lines limit the region in which the flow field measurements are less accurate. a) Typical flow field. The length of the arrows is proportional to local velocity. Not all data points of the field are plotted for clarity. Dashed line indicates the free surface. Also shown is the fitted shape of yield surfaces (see text). b) Maximum shear strain rate at a stage where flow is symmetric. c) Time and space average of the maximum shear strain rate (lower inset) correlates to vertical steps at the surface (upper inset). d) Fit for each shear band according to eq. (1).

Features of the observed flow through the back and front surface of the cell are well correlated showing that it is nearly two dimensional. The measured velocity field reveals a flow that originates below the fingers' tip, at a distance comparable to its radius, and extends up to the free surface within a region whose lateral extension is of the order of ζ. Outside this region the material is at rest (fig. 2a). We characterize yield surfaces geometrically with the maximal shear strain rate field [14], $\dot{\gamma}_{max} = \sqrt{\dot{\epsilon}_{xy}^2 + \frac{1}{2}\left(\dot{\epsilon}_{yy} - \dot{\epsilon}_{xx}\right)^2}$. Here $\dot{\epsilon}_{\alpha\beta} = \frac{1}{2}\left(\frac{\partial u_\alpha}{\partial x_\beta} + \frac{\partial u_\beta}{\partial x_\alpha}\right)$ is the strain rate tensor and u_α is the velocity ($\alpha = 1$, horizontal component, $\alpha = 2$, vertical, positive downwards, component). This representation shows that the fluidized and stagnant regions are separated by two shear bands (fig. 2b) that focus shear and vorticity [9].

The flow evolves in a non-regular way as the finger moves downwards. Indeed, from time to time, stagnant material suddenly sticks to the moving one and starts to flow. At the same time a new shear band is created underneath the first one, leading to a scenario where shear bands virtually jump alternately at either side of the finger towards increasing depth. Between such events shear bands gradually change their shape. This behavior is characteristic of dense granular materials in which non-moving grains are in jammed states. Features of the flow manifest at the free surface by a characteristic swelling, which exhibits well defined jumps that, despite the fluctuations on shear bands, are relatively well correlated with the average maximum shear (fig. 2c). Interestingly, the surface structure presented here shares some similarities with multi-ring impact basins [8] observed on the surfaces of almost all planetary bodies in the Solar System that have solid crusts. The details of their formation mechanism are still unclear although it is believed that plastic failure is responsible of such characteristic pattern of faults.

Let us now describe the dynamics of the flow in terms of the Mohr-Coulomb yield criterion, which states that the material is locally at incipient failure if $\sigma_t - \sigma_n \tan\phi = c$ [3]. Here σ_t and σ_n are respectively the shearing and compressive stresses at the yielding surface, ϕ is the angle of friction of the material and c is the cohesion of the material, which we neglect. In this model the onset of slipping occurs at a critical shear stress $\sigma_c = \sigma_n \tan\phi$, while the slipping angle, ϕ_0, relative to the local maximum principal direction of stress, is given by $\phi_0 = \pm(\pi/4 + \phi/2)$. According to [12] and references therein, a penetrating finger with a semicircular tip induces a near-tip stress field whose local principal directions are radial and azimuthal, the origin being the geometrical center O of the semicircular tip. In this region the effects of gravity are small. Due to symmetry of the system the material might fail right below the tip at either positive or negative values of ϕ_0. This is the starting point of the yield surfaces. By continuation these surfaces must intersect the radial principal lines at the same angle ϕ_0. The only curve satisfying this condition is a logarithmic spiral

$$\rho(\theta) = \rho_0 \exp(\theta/\tan\phi_0), \qquad (1)$$

where (ρ, θ) are polar coordinates centered at O (θ is measured relative to the vertical, positive downwards, direction). Parameter ρ_0 represents the distance from O at which shear bands start. To perform our analysis, at each stage we fit the local maxima of $\dot{\gamma}_{max}$ (fig. 2b) with logarithmic spirals, using ρ_0 and ϕ_0 as free parameters.

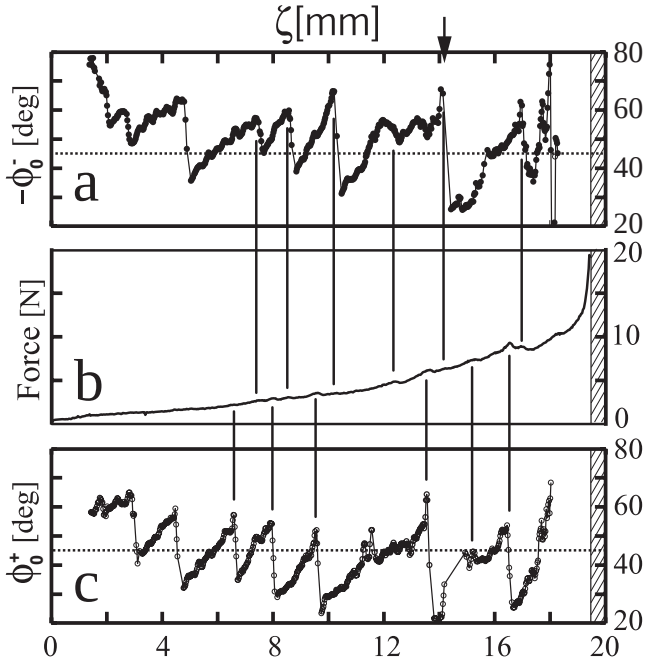

FIG. 3: Parameter ϕ_0 for spiral-shaped yield surfaces (eq. 1) and vertical force applied to the finger, as a function of penetration depth ζ. Dashed regions indicate bottom of the cell. Arrow indicates the distance at which shear bands might touch the container bottom.a) Left spiral. b) Force drops correlated to jumps in parameter ϕ_0. c) Right spiral. a) and c) Dashed line corresponds to plastic yielding (see text).

The fit leads to continuous changes in ϕ_0 (fig. 3), while successive values of parameter ρ_0 do not show appreciable variations. Indeed, ρ_0 is always comprised between the radius R of the finger and the value corresponding to plastic failure (see below). This fact is confirmed by direct observation of a small wedge-shaped region underneath the finger where grains move at the same speed of the finger. The quality of the fit is evidenced by fig. 2d. Matching with a spiral is satisfactory until shear bands reach the regions where gravity is dominant. Here the medium is close to the "passive" state described by Rankine [3] and the material slides at a nearly constant angle relative to the vertical. We conclude that yield surfaces nucleate always at nearly the same distance from the moving finger but may experience important changes in shape. Predicted yielding angles for the granular material are not equal to 45° with respect to principal axis, as would be the case for a plastic material where yielding is controlled solely by shear. Our experimental results in fig. 3 show a stick-slip type dynamics where the magnitude of the angle ϕ_0 is always increasing linearly as the finger plunges into the granular material, but jumps to a lower value at a shear band nucleation event. For yield surfaces relatively far from the bottom of the cell, ϕ_0 oscillates around 45°.

Since at a shear band nucleation event, ϕ_0 is about $\pi/6$ (fig. 3), an acceptable solution exists only if the maximum principal axis is coincident with the azimuthal direction. Then $\phi \approx \pi/6$. Once a shear band has nucleated, the increment of ϕ_0 with finger penetration can not be captured by this static approach. However, shear bands keep spiral shapes, characteristic of a well defined yielding angle, suggesting that a generalized yielding criterium might hold for the post failure state.

We address now the problem of the dynamics associated to the observed flow. Consider first the effect of the side walls and bottom of the cell. The pushing finger induces consolidation of the material in the non-flowing regions. This is evidenced by the existence of a small downward compression under the shear bands, described in [9]. If the material becomes highly compact the presence of the walls is "screened" by the consolidated material. Hence after a transient the system should behave indistinctly shall it be infinite or finite. Notice that hydrostatic effects are very small if compared to the load imposed by the pushing finger. On the other hand, the nucleation, structure and evolution of shear bands is determined by the stress distribution. To get an idea on the stresses involved in the process we simultaneously measure the force that the finger applies to the granular material (fig. 3b). To dismiss possible friction effects between the finger and the glass plates we measured the penetration force in an empty cell (no beads). The force was less than $(0.06 \pm 0.01)[N]$. Another effect is the friction experienced by beads in contact with the glass plates. The involved forces should be small, for the system, being considerably thick in comparison to particle size, is not transversally frustrated. The method of characteristics [3] predicts a transverse pressure smaller than the surcharge, but of the same order. Friction resulting from transverse pressure applied on a surface of size $\sim R^2$ compared to the surcharge of the finger, acting on a surface of size $\sim RL$ (L is the width of the cell), is smaller than the measured vertical force by a factor $\sim \mu\frac{R}{L}$, where μ is the friction coefficient between a bead and the glass. While the finger moves at constant speed, the force increases smoothly but experiences occasional drops which are correlated to shear band jumps, as can be seen from fig. 3. One may infer from the same figure that the force repeatedly jumps towards branches associated to flow patterns requiring less driving force. Analogous stick-slip behavior described in [15] might obey to the same mechanism. A similar idea has been used for stationary flow in a partially rotating container [16] filled with granular material. Starting from a least dissipation hypothesis, the authors predict the shape of the shear surfaces the system naturally develops.

It is well known that yielding is accompanied by dilation in the regions where shear occurs. Otherwise the system would not flow. We therefore study the dilation undergone by the granular material. It can be evidenced from the divergence of the velocity field, $\nabla \cdot \vec{u} = \dot{\epsilon}_{xx} + \dot{\epsilon}_{yy}$.

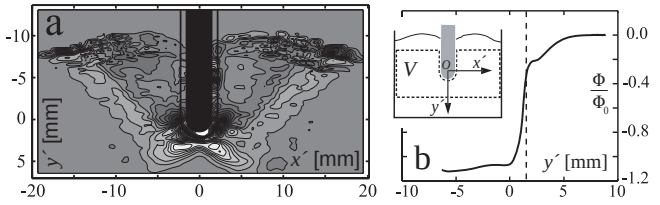

FIG. 4: a) Divergence of the flow field, $\nabla \cdot v = v_{xx} + v_{yy}$, averaged over 200 stages of penetration, in the reference frame of the moving finger. White (black) regions indicate dilation (compaction). b) Total vertical flow integrated over successive horizontal sections, averaged over the same 200 stages of penetration, normalized to the imposed flow, $\Phi_0 = 2R\nu$. Dashed line indicates the vertical position of the tip of the finger. Inset: Lagrangian volume V (dashed contour).

It is convenient to consider the equivalent problem of a fixed finger put inside a constant vertical flow and compute average fields over successive stages, in a reference frame fixed to the finger. Divergence is highly sensitive to experimental error, for density fluctuations constitute a weak effect. Despite this, regions where $\nabla \cdot \vec{u} \neq 0$ are noticeable. They are located in the shear bands (fig.4a), especially at their starting point. Consider the moving frame depicted in fig. 4b (inset) and define the lagrangian volume V (same figure). For the sake of simplicity, in the following all quantities are defined per unit of thickness. The instantaneous rate of dilation of volume V is given by $\frac{dV}{dt} = \int_V (\nabla \cdot \vec{v}) dV$, where $\vec{v}$ is the velocity field in the reference frame of the finger. To interpret our results we will assume a stationary, in average, flow relative to the finger. Substitution of $\vec{v} = \vec{u} - \nu\hat{j}$ and $\frac{dV}{dt} = \nu \frac{dV}{d\zeta}$ leads, after use of the divergence theorem, to

$$\frac{dV}{d\zeta} = -2R\left(1 + \frac{\Phi(y')}{\Phi_0}\right), \qquad (2)$$

where $\Phi(y') = \int u_2(x', y')dx'$ and Φ_0 is the volume removed by the finger per unit of time. We note that $\Phi(y')/\Phi_0 = -1$, if the material were incompressible, provided that $y' < 0$.

From fig. 4b, $\Phi(y')/\Phi_0 \approx -1.1$ for $y' < 0$, hence dilation rate is nearly constant and approximately equal to $0.3mm^2$ per mm of penetration. On the other hand, direct measurement of the area of the midplane section of granular material, where vertical velocity is maximum along the transverse direction, shows a linear growth rate of $1.7mm^2$ per mm of penetration. The former and latter values constitute, respectively, lower and higher bounds for the actual dilation rate. A rough estimate, considering only the mobilized material (initially at rest), for $\zeta = 10mm$, gives a corresponding global dilation lying in the range $3\% - 15\%$. We note that in a granular material the transition from a random close packing (rcp) to a random loose packing (rlp) corresponds to a dilation of about 20%. Our results are consistent with the initial conditions of the experiment where an intermediate packing fraction is expected.

In summary, we have visualized and measured quasi planar flow fields in a granular material around a moving rigid object via a standard image cross-correlation method. Although our measurements are performed at the interface between grains and a retaining glass plate, our results provide a precise idea of the geometry of shear bands and their dynamics. This should prove useful in understanding sources of dilation, compaction and yielding in granular materials, but also in metallic glasses [17] and crater formation [8], where correlation of free surface striation with bulk flow might provide useful information.

This work was supported by Conicyt-Chile under research program Fondap N^o 11980002.

[1] Jaeger, H. M., Nagel, S. R. and Behringer, R. P., Rev. Mod. Phys **68**, No. 4, 1259–1273 (1996).
[2] de Gennes, P. G., Rev. Mod. Phys. **71**, No. 2, 374–382 (1996).
[3] Nedderman, R. M., Cambridge University Press (1992).
[4] Kolb, E., Cviklinski, J., Lanuza, J., Claudin, P. and Clément, E., Phys. Rev. E **69**, 031306 (2004).
[5] Stone, M. B., Barry, R., Bernstein, D. P., Pelc, M. D., Tsui, Y. K. and Schiffer, P., Phys. Rev. E **70**, 041301 (2004).
[6] Geng, J. and Behringer, R. P., Phys. Rev. E **71**, 011302 (2005).
[7] Gill, D. R. and Lehane, B. M., Geotechnical Testing Journal, GTJODJ **24**, No. 3, 324–329 (2001).
[8] For a review, see for instance, Melosh, H. J. and Ivanov, B. A., Annu. Rev. Earth Planet. Sci. **27**, 385–415 (1999).
[9] Hamm, E. and Melo, F.(2005), Europhys. Lett. **73** (3), 356–362 (2006)
[10] Mueth, D. M., Debregeas, G. F., Karczmar, G. S., Eng, P. J., Nagel, S. R. and Jaeger, H. M., Nature, **406**, 385-389 (2000).
[11] Tsai, J. C., Voth, G. A. and Gollub, J. P., Phys. Rev. Lett., **91**, 064301 (2003).
[12] Oda, M. and Iwashita, K. Mechanics of granular materials., A. A. Balkema, 1999.
[13] Hill, J. and Wu, Y.-H., Q. Jl. Mech. Appl. Math, **49**, Pt. 1, 81–105 (1996).
[14] Landau, L. and Lifchitz, E., Théorie de l'Élasticité, 2ème Édition, 1990, Mir.
[15] Albert, R., Pfeifer, M., Barabási, A. L. and Schiffer, P., Phys. Rev. Lett. **82**, No. 1, 205–208 (1999).
[16] Unger, T., Török, J., Kertész, J., Wolf, D. E., Phys. Rev. Lett. **92**, No. 21, 214301 (2004).
[17] Schuh, C. and Lund, A., Nature Mat. **2**, July, 449–452 (2003).